MOLECULAR AND CELLULAR BIOLOGY, Mar. 2001, p. 1573–1580 Vol. 21, No. 5
0270-7306/01/$04.00+0 DOI: 10.1128/MCB.21.5.1573–1580.2001

VAMP3 Null Mice Display Normal Constitutive, Insulin- and Exercise-Regulated Vesicle Trafficking

CHUNMEI YANG,[1] SILVIA MORA,[1] JEFFREY W. RYDER,[1] KENNETH J. COKER,[1]†
POLLY HANSEN,[2] LEE-ANN ALLEN,[3] AND JEFFREY E. PESSIN[1]*

Department of Physiology and Biophysics[1] and Department of Internal Medicine,[3] The University of Iowa, Iowa City, Iowa 52242, and Department of Cell Biology, Pfizer Global Research and Development, Ann Arbor, Michigan 48105[2]

Received 19 September 2000/Returned for modification 28 September 2000/Accepted 27 November 2000

To investigate the physiological function of the VAMP3 vesicle SNARE (v-SNARE) isoform in the regulation of GLUT4 vesicle trafficking, we generated homozygotic VAMP3 null mice by targeted gene disruption. The VAMP3 null mice had typical growth rate and weight gain, with normal maintenance of fasting serum glucose and insulin levels. Analysis of glucose disposal and insulin sensitivity demonstrated normal insulin and glucose tolerance, with no evidence for insulin resistance. Insulin stimulation of glucose uptake in isolated primary adipocytes was essentially the same for the wild-type and VAMP3 null mice. Similarly, insulin-, hypoxia-, and exercise-stimulated glucose uptake in isolated skeletal muscle did not differ significantly. In addition, other general membrane trafficking events including phagocytosis, pinocytosis, and transferrin receptor recycling were also found to be unaffected in the VAMP3 null mice. Taken together, these data demonstrate that VAMP3 function is not necessary for either regulated GLUT4 translocation or general constitutive membrane recycling.

Insulin increases glucose uptake in adipose and striated muscle tissues primarily by recruiting the GLUT4 glucose transporter protein to the cell surface (37). In the basal non-insulin-stimulated state, the majority of GLUT4 resides in one or more intracellular compartments (44, 45). Upon addition of insulin, the signaling cascade triggered by the insulin receptor leads to rapid translocation of the GLUT4 transporter to the plasma membrane, thereby increasing the number of transporters at the cell surface and the rate of glucose uptake (12, 27, 38, 41).

The process of GLUT4 translocation shares important features with the exocytosis of synaptic vesicles during neurotransmitter release. For example, the plasma membrane docking and fusion of GLUT4 vesicles appears to require the t-SNARE protein isoforms syntaxin 4 and SNAP23 (9, 37, 48). GLUT4 vesicles contain the v-SNARE-interacting partners VAMP2 and VAMP3, both of which translocate to the plasma membrane in parallel with GLUT4 (33, 47). Recent studies using various toxins and endosomal ablation techniques have indicated that VAMP2 is the predominant v-SNARE responsible for insulin-stimulated GLUT4 translocation in cultured 3T3-L1 adipocytes and in the L6 muscle cell line (9, 32, 33, 40). In contrast, guanosine-5′-*O*-(3-thiotriphosphate) (GTPγS)-stimulated GLUT4 translocation was found to be dependent on VAMP3, thereby suggesting the presence of two independently regulated pools of GLUT4 storage compartments (35). In this regard, skeletal muscle has also been shown to contain two pools of GLUT4 vesicles, one that responds to insulin and another that is responsive to exercise and contraction (1, 11, 39). In addition, the skeletal muscle exercise-contraction subpopulation utilizes a signaling pathway independent of the phosphatidylinositol (PI) 3-kinase (30, 31, 50). Similarly, GTPγS stimulation in adipocytes is also independent of the PI 3-kinase, suggesting that the GTPγS and exercise-contraction pathways may utilize the same populations of intracellular GLUT4 vesicles (18).

In addition to the potential role in GLUT4 translocation, VAMP3 has also been suggested to play an important functional role in phagocytosis and general receptor membrane trafficking events (5, 14, 22, 34). Thus, to address the relative contributions of VAMP3 in insulin- and exercise-contraction-stimulated GLUT4 translocation, glucose uptake, and general membrane trafficking processes, we have generated mice with a homozygotic disruption of the VAMP3 gene. In this report, we characterize these mice and demonstrate that they are phenotypically normal in terms of glucose homeostasis, tissue glucose transport, pinocytosis, and general membrane receptor recycling.

MATERIALS AND METHODS

Isolation of murine VAMP3 genomic clones. The full-length 0.4-kb murine VAMP3 cDNA containing the 312-bp open reading frame (kindly provided by Amira Klip, The Hospital for Sick Children, Toronto, Ontario, Canada) was sequenced to confirm the identity of the clone. A panel of PCR oligonucleotide primers encompassing the entire VAMP3 cDNA (designated A to J) was designed. All 10 possible primer combinations were tested by PCR amplification of the murine cDNA clone and yielded products of the expected sizes. Subsequent PCR amplification of mouse liver DNA using the VAMP3 pair H (5′-TGA AACAAGTGCTGCCAAGT)-J (5′-CGATGATGATGATGACAATG) primer pair yielded a product of 965 bp, much larger than the 104-bp H-J product from the cDNA, indicating the presence of intronic sequences. The genomic H-J product was subcloned and sequenced, and its identity as part of the mouse VAMP3 gene was confirmed by BLAST analysis. The H and J primers were then sent to Genome Systems (St. Louis, Mo.), where a PCR-based screen of a murine 129/Sv/J library yielded a ~120-kb bacterial artificial chromosome clone containing the VAMP3 gene. Based on Southern blot analysis of this clone, 15 kb of the genomic sequence was subcloned and extensively analyzed. This 15-kb fragment

* Corresponding author. Mailing address: Department of Physiology and Biophysics, The University of Iowa, Iowa City, IA 52242. Phone: (319) 335-7823. Fax: (319) 335-7886. E-mail: Jeffrey-Pessin@uiowa.edu.

† Present address: Lexicon Genetics Incorporated, The Woodlands, TX 77381.

contains the entire VAMP3 gene, which has five exons and spans approximately 10 kb of genomic sequence (accession numbers AF308433 and AF308434).

Generation of the VAMP3 targeting vector. The VAMP3 targeting vector was constructed by using a positive-negative selection vector, pOSDUPDEL (obtained from the Gene Targeting Laboratory, The University of Iowa, Iowa City). The 5′ homologous region in the targeting vector was a 2.3-kb *Spe*I-*Bgl*II fragment containing intron 1, exon 1 (which ends with AT of the start codon ATG), and upstream sequences of the VAMP3 gene. This fragment was inserted into the pOSDUPDEL vector in the *Xba*I-*Bam*HI cloning site downstream of the neomycin phosphotransferase gene (*neo*) cassette. Orientation of this fragment was confirmed by restriction enzyme digestion and sequencing. To generate the 3′ homologous region, the 3.3-kb *Bgl*II-*Bgl*II fragment containing a portion of intron 3, exon 4 and 5, 3′ untranslated region, and downstream sequences was isolated and inserted into the vector in the *Bcl*I cloning site upstream of the *neo* cassette. Orientation of this fragment was also confirmed by restriction enzyme digestion and sequencing. The vector contained a thymidine kinase cassette distal to the 5′ homologous region. The mutant gene therefore lacked a 7.8-kb region which included 636 bp of intron 1, exon 2 (containing guanosine of the start codon ATG), intron 2, exon 3 (encoding the entire coiled-coil domain of VAMP3), and 442 bp of intron 3.

Generation of VAMP3 null mice. The targeting construct was linearized with *Pme*I and introduced into 2×10^7 pluripotent embryonic stem (ES) cells (R1 clone) by electroporation (Gene Pulser; Bio-Rad, Hercules, Calif.). ES clones that were G418 and ganciclovir resistant were isolated, amplified, and screened for targeting fidelity by Southern blot analysis (see Fig. 1B). Seventeen targeted clones were obtained from 95 analyzed. Six of these clones were subsequently reconfirmed by Southern blot analysis, and the single targeting event was also confirmed by hybridizing the *Xba*I-digested ES DNA with a *neo* probe. Cells from two targeted clones (AA30 and AA60) were microinjected into donor C57BL/6J blastocysts and implanted into pseudopregnant ICR females. Chimeric animals resulting from the microinjections were bred to C57BL/6J mice, and agouti pups were screened for germ line transmission of the mutant allele. The genotypes from these matings and all subsequent matings were determined by PCR on DNA from tail biopsy specimens. All experimental analyses were performed on matched littermates from hybrid C57BL/6-129/Sv/J backgrounds. All mice were housed in the animal care unit of the University of Iowa College of Medicine according to animal care guidelines.

Western blot analysis. Tissue extracts were prepared by dissection and homogenization in lysis buffer (25 mM HEPES [pH 7.4], 1% NP-40, 137 mM NaCl, 1 mM phenylmethylsulfonyl fluoride, 10 μg of aprotinin/ml, 1 μg of pepstatin/ml, 5 μg of leupeptin/ml, 5 mM benzamidine) in a Polytron PT-10 homogenizer. The samples were then centrifuged at $2{,}000 \times g$ for 5 min, and the supernatant was recentrifuged at $14{,}000 \times g$ for 20 min at 4°C. Total fat membranes were prepared by homogenizing white fat tissue in HES buffer (255 mM sucrose, 20 mM HEPES [pH 7.4], 1 mM EDTA), centrifugation at $800 \times g$ for 4 min, and recentrifugation of the supernatant at $180{,}000 \times g$ for 70 min at 4°C. Proteins were resolved by sodium dodecyl sulfate-polyacrylamide gel electrophoresis on 3 to 15% linear gradient gels and subjected to immunoblotting. The sources of antibodies against proteins indicated in Fig. 2 were described previously (28, 46).

Metabolic measurements. Fed and fasted (12 h) blood glucose measurements were determined with a glucometer (De Centech, St. Paul, Minn.). Serum insulin was determined by enzyme-linked immunosorbent assay, using mouse insulin as a standard (ALPCO, Windham, N.H.). Serum triglyceride, nonesterified free fatty acid, and cholesterol concentrations were determined by colorimetric assay (WAKO Chemicals, Richmond, Va.).

GTT and ITT. Glucose tolerance tests (GTTs) were performed on mice fasted for 12 h. D-Glucose (20% solution, 2 g/kg of body weight) was injected intraperitoneally into the animals, and blood glucose values were measured at 0, 30, 60, 90, and 120 min postinjection. Insulin tolerance tests (ITTs) were performed on mice fasted for 6 h. Animals were injected intraperitoneally with Humulin R (0.75 U/kg of body weight; Eli Lilly Corp., Indianapolis, Ind.), and blood glucose values were determined immediately before and at 15, 30, and 60 min after injection.

Glucose uptake in primary adipocytes. The transport of glucose was determined using 2-deoxyglucose as previously described (19). Briefly, adipocytes were isolated from epididymal fat pads by collagenase (2 mg/ml) digestion at 37°C with constant agitation in Krebs-Ringer buffer containing 15 mM sodium bicarbonate, 10 mM HEPES, 2 mM sodium pyruvate, 200 nM adenosine, and bovine serum albumin (BSA; 2.5%, wt/vol). The cells were then incubated with or without 100 nM insulin for 30 min, and 2-deoxy-D-[^{3}H]glucose (final concentration, 0.1 mM; ICN, Costa Mesa, Calif.) was then added for 10 min. The reaction was terminated by a 30-s spin over dinonylphthalate oil, and the incorporated radioactivity in the cells was counted. Nonspecific uptake and trapping in the extracellular space was determined by measuring uptake in the presence of cytochalasin B.

Insulin-stimulated glucose transport in isolated skeletal muscle. Soleus muscles were isolated for incubation in vitro, and the transport assay was performed as described previously (23). Unless stated otherwise, all incubation media were prepared from a pregassed (95% O_2–5% CO_2) stock of Krebs-Henseleit bicarbonate buffer (KHB) supplemented with 5 mM HEPES and 0.1% BSA (radioimmunoassay grade). The muscles were incubated in a shaking water bath (30°C) for 30 min in 1 ml of KHB supplemented with 5 mM glucose and 15 mM mannitol in the absence or presence of 120 nM insulin. The muscles were then incubated for 10 min in glucose-free medium. Thereafter, muscles were transferred to vials containing 1 mM [^{3}H]2-deoxyglucose (2.5 μCi/ml) and 19 mM [^{14}C]mannitol (0.7 μCi/ml) and incubated for 20 min. The muscles were dissolved with 0.5 M NaOH, and 2-deoxyglucose uptake was assessed as described by Hansen et al. (23).

Hypoxia-stimulated glucose transport. Soleus muscles were removed for incubation under normoxia or hypoxia, without or with the addition of insulin. Hypoxic medium was pregassed with 95% N_2–5% CO_2. Muscles were preincubated under either normoxic (95% O_2–5% CO_2) or hypoxic (95% N_2–5% CO_2) conditions for 45 min (30°C) in KHB supplemented with 5 mM D-glucose and 15 mM mannitol. The specific gas mixture was maintained throughout the preexposure period. Following preincubation, muscles were transferred to oxygenated KHB containing 2 mM pyruvic acid and 18 mM mannitol. Muscles were incubated for 15 min at 30°C under a gas phase of 95%O_2–5%CO_2 and 2-deoxyglucose uptake was measured as described above.

Exercise-induced glucose transport. Mice were exercised by swimming as described by Ryder et al. (43). Briefly, the mice were randomly assigned to a sedentary or exercised group and placed in plastic barrels measuring 45 cm in diameter and filled to a depth of ~40 cm. Water temperature was maintained at 34 to 35°C. Mice swam for six 30-min intervals separated by 5-min rest periods. After the last swim interval, mice were anesthetized, and extensor digitorum longus (EDL) muscles were removed immediately and incubated for 15 min in 1 ml of KHB supplemented with 20 mM mannitol. 2-Deoxyglucose uptake was determined as described above.

Macrophage and bacterial cultures. Bone marrow-derived macrophages (BMMs) were differentiated from marrow extracted from the femora of male and female wild-type or VAMP3 null mice in medium containing HEPES-RPMI 1640, 15% heat-inactivated fetal bovine serum (FBS), 1% L-glutamine, 100 U of penicillin G/ml, 100 μg of streptomycin/ml, and 20% L-cell conditioned medium (a source of colony-stimulating factor 1 [CSF-1]). Mature BMMs were used after a total of 7 to 19 days in culture. For each experiment, BMMs were scraped off petri dishes and replated on coverslips or in tissue culture dishes as indicated. Twelve to 24 h after plating, BMM were switched to minimal essential medium alpha containing 10% heat-inactivated FBS and 1% L-glutamine (without antibiotics or CSF-1) and incubated overnight at 37°C prior to use. *Helicobacter pylori* strain 11637 was cultured on Trypticase soy agar plates containing 5% sheep blood under microaerophilic conditions as previously described (3).

Phagocytosis assays. Macrophages were plated on acid-washed round glass coverslips (12-mm diameter; Fisher, Pittsburgh, Pa.) in complete medium and then starved of CSF-1 and antibiotics as indicated above. Unopsonized zymosan particles and zymosan particles opsonized with complement were prepared as described elsewhere (2); immunoglobulin G (IgG)-opsonized zymosan particles were prepared using Molecular Probes opsonizing reagent according to the manufacturer's specifications. One-micrometer-diameter latex beads were the generous gift of Larry Schlesinger, Department of Medicine, University of Iowa. Washed *H. pylori* and other particles were dispersed in tissue culture medium to achieve a ratio of 3 zymosan particles, 10 latex beads, or 25 bacteria per macrophage. For all experiments, phagocytosis was synchronized by centrifugation as previously described (2, 3). Intracellular and extracellular cell-associated bacteria were determined as previously described by immunofluorescence labeling with *H. pylori* polyclonal antibodies (24). For all particles, BMMs that had ingested zymosan, opsonized zymosan, or latex beads for 30 min at 37°C were fixed in 10% buffered formalin and permeabilized in −20°C acetone (4). Fixed cells were blocked overnight at 4°C in Dulbecco's phosphate-buffered saline containing 0.5 mg of NaN_3/ml, 5 mg of BSA/ml, and 10% horse serum (blocking buffer). Cell-associated zymosan, opsonized zymosan, and latex beads were detected by phase-contrast optics. Internalized particles were identified by staining fixed and permeabilized cells with monoclonal antibodies to lamp-1 (Developmental Studies Hybridoma Bank, University of Iowa) and secondary antibodies conjugated to fluorescein isothiocyanate (goat anti-rat IgG; Jackson ImmunoResearch Laboratories, West Grove, Pa.) Washed coverslips were mounted on glass slides in Mowiol, and fluorescence was visualized using a Zeiss Axioplan2 microscope

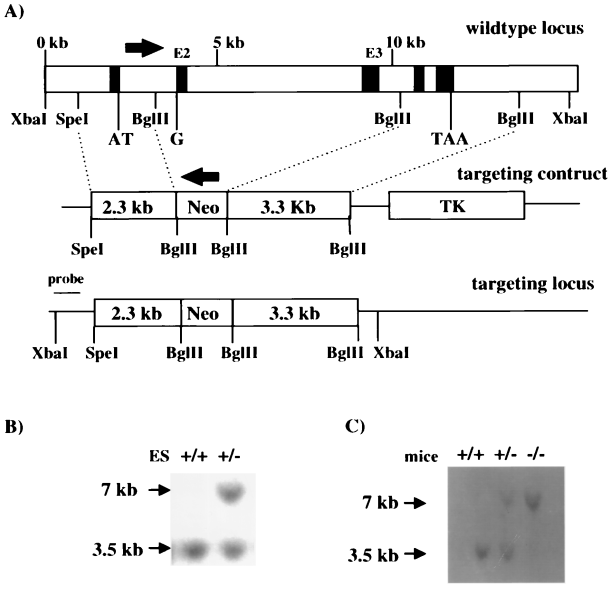

FIG. 1. Generation of VAMP3-deficient mice by homologous recombination in ES cells. (A) Schematic representation of the wild-type murine *VAMP3* locus, the targeting construct, and the targeted locus. A 7.8-kb region including exon 2 (E2) and exon 3 (E3) (black boxes) was replaced by a *neo* cassette inserted in the reverse orientation. The 5′ and 3′ homologous regions of the targeting construct were 2.3 and 3.3 kb, respectively. TK, thymidine kinase. Southern blots show genomic DNA extracted from ES cells (B) and mouse tail (C), using a diagnostic probe (as indicated in panel A). The wild-type locus generates a 3.5-kb *Xba*I fragment, whereas the targeted allele produces a 7-kb *Xba*I fragment.

(Carl Zeiss, Inc., Thornwood, N.Y.). For each experiment, at least 100 infected macrophages were counted on triplicate coverslips.

Transferrin receptor recycling. Primary mouse embryonic fibroblasts were isolated from wild-type or VAMP3-deficient mice following standard procedures (25). Cells were maintain in Dulbecco modified Eagle medium containing 15% FBS. The transferrin recycling assay was performed as previously described by Ceresa et al. (8). Briefly, 35-mm-diameter dishes of cells were depleted of bovine transferrin and then incubated with [^{125}I]transferrin (3 nM; 1 μCi/μg) at 4°C for 2.5 h. Unbound ligand was removed by washing the cells with serum-free medium at 4°C, and internalization was initiated by warming the cells to 37°C. At various times, endocytosis was blocked by washing the cells with ice-cold phosphate-buffered saline. The amount of ligand cell surface bound (acid dissociable), in the medium (recycled), and internalized (cell-associated acid resistant) was measured by counting on a Packard Autogamma 5000 counter.

Pinocytosis. The fluid-phase uptake of horseradish peroxidase (HRP) was assayed as described by Daro et al. (13). Briefly, primary mouse embryonic fibroblasts from wild-type or VAMP3-deficient mice were labeled with 2.5 mg of HRP/ml Dulbecco modified Eagle medium in DMEM supplemented with 2 mg of BSA/ml for various times. Cells were then washed extensively, lysed in 1% Triton X-100, assayed for HRP activity, and normalized to total cell protein.

RESULTS

Generation of VAMP3-deficient mice. We initially constructed a targeting vector in which 7.8 kb of VAMP3 genomic sequence, including exon 2, which contains the guanosine of the start codon ATG, and exon 3, which encodes the entire coiled-coil domain of VAMP3, was replaced with a *neo* cassette oriented in the opposite direction as the endogenous VAMP3 gene (Fig. 1A). Of 95 neomycin-resistant ES clones analyzed, 17 demonstrated the desired mutation, as confirmed by Southern blot analysis (shown for one clone in Fig. 1B). Two of these clones were used to generate chimeric founder mice. Heterozygotic mice from the F_1 generation were identified by PCR analysis (data not shown) and were crossed to obtain VAMP3-deficient mice. VAMP3-deficient mice were born from heterozygous matings in a predicted Mendelian inheritance frequency. Figure 1C shows an example of a Southern blot analysis of the VAMP3 locus of wild-type, heterozygous, and homozygous mutant mice.

To confirm that VAMP3 protein was not present in the VAMP3-deficient mice, we performed Western blot analysis of several tissues from wild-type, heterozygous, and VAMP3-deficient animals (Fig. 2). The VAMP3 protein is ubiquitously expressed and found in all tissues examined. However, expres-

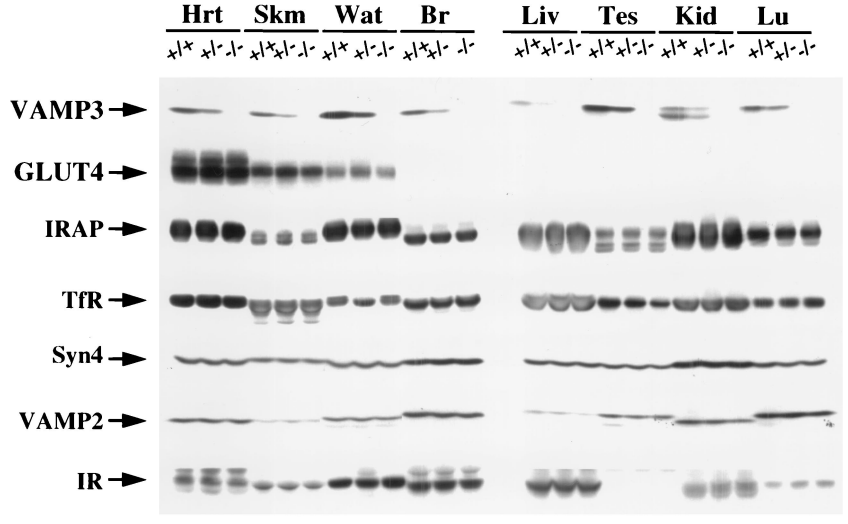

FIG. 2. VAMP3-deficient mice do not express VAMP3 but maintain normal expression levels of GLUT4 and other related proteins. Tissue extracts from heart (Hrt), skeletal muscle (Skm), white adipose tissue (Wat), brain (Br), liver (Liv), testis (Tes), kidney (Kid), and lung (Lu) were separated by sodium dodecyl sulfate-polyacrylamide gel electrophoresis and immunoblotted for VAMP3, GLUT4, insulin-responsive aminopeptidase (IRAP), transferrin receptor (TfR), syntaxin 4 (Syn4), VAMP2, and insulin receptor (IR).

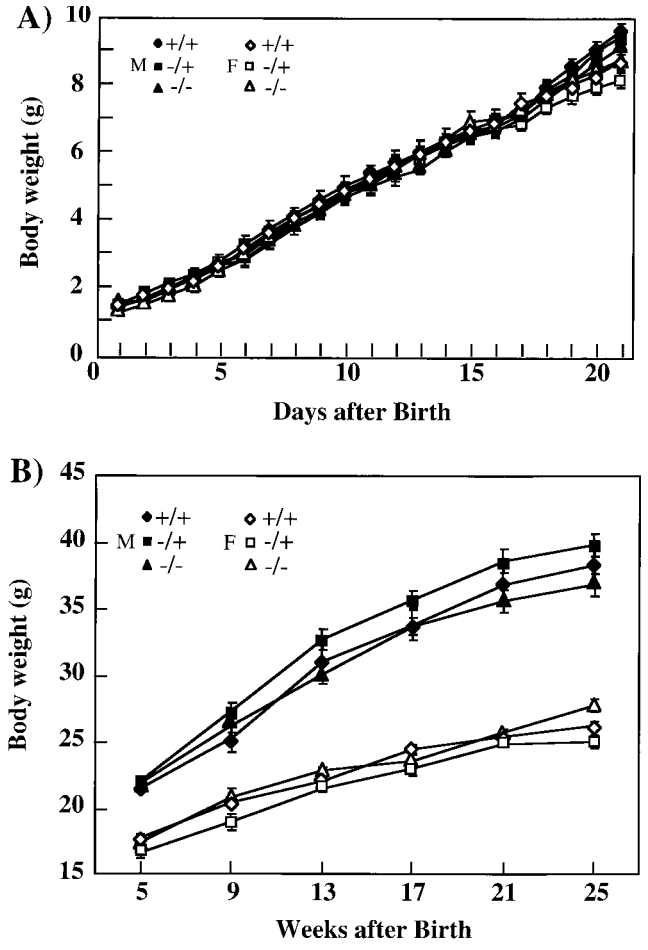

FIG. 3. Deletion of the VAMP3 gene does not affect growth of VAMP3-deficient mice. Female (F) and male (M) offspring from heterozygous breedings were weighed every day from days 1 to 21 (A) and thereafter every 4 weeks from weeks 5 to 25 (B).

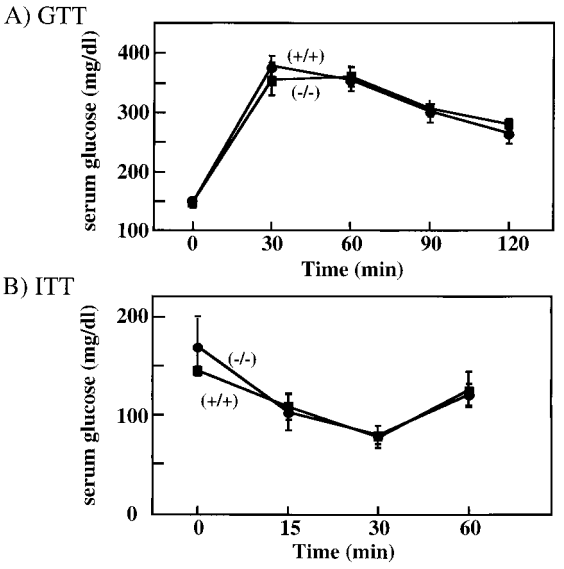

FIG. 4. VAMP3-deficient mice display normal glucose and insulin tolerance. (A) GTT of 16-week-old male mice. D-Glucose (20% solution, 2 g/kg of body weight) was injected intraperitoneally into mice fasted for 12 h. Blood glucose was measured at 0, 30, 60, 90, and 120 min postinjection using a glucometer as described in Materials and Methods. (B) ITT of 16 week-old male mice. Insulin (0.75 U/kg of body weight) was injected intraperitoneally to mice that were fasted for 6 h. Blood glucose was measured immediately before and at 15, 30, and 60 min after injection as described in Materials and Methods. The experimental groups consisted of 10 and 6 mice for GTT and ITT, respectively, and were performed a minimum of three times with similar results.

sion was consistently 50% less in all tissues of the heterozygous knockout mice and was eliminated in the VAMP3-deficient mice. Furthermore, the loss of VAMP3 protein expression was not compensated for by changes in several other SNARE proteins, proteins localized to GLUT4 vesicles, and other general endosome trafficking proteins. These data demonstrate that this conventional genomic replacement results in the complete ablation of VAMP3 protein expression without any specific compensatory changes in protein expression.

Development and metabolic profiles of VAMP3-deficient mice. The VAMP3-deficient mice displayed growth and weight gain characteristics identical to those of wild-type littermates (Fig. 3). Although the older male mice maintain a greater body weight than female mice, there was no discernible difference between the wild-type, heterozygotic, and homozygotic knockout animals. Similarly, all metabolic parameters assessed (serum glucose, insulin, triglyceride, free fatty acids, and cholesterol) were not significantly different between the wild-type and VAMP3 null mice in either the fed or fasted state (Table 1).

VAMP3-deficient mice display normal glucose tolerance. Since VAMP3 has been implicated in certain aspects of GLUT4 translocation, we next examined the ability of these mice to respond to a glucose challenge (Fig. 4A). Following a single intraperitoneal bolus injection of glucose, circulating glucose levels maximally increased at 30 min and slowly declined over the next 90 min. Essentially identical glucose tol-

TABLE 1. Metabolic characteristics of wild-type and VAMP3 null mice[a]

Mice	Concn in serum									
	Glucose (mg/dl, $n = 9$)		Insulin (ng/ml, $n = 9$)		Triglycerides (mg/dl, $n = 7$)		Free fatty acids (mM, $n = 7$)		Cholesterol (mg/dl, $n = 7$)	
	Fed	Fasted	Fed	Fasted	Fed	Fasted	Fed	Fasted	Fed	Fasted
Wild type	158 ± 10	110 ± 8	1.92 ± 0.29	0.38 ± 0.07	130.2 ± 16	88.1 ± 13	0.42 ± 0.04	0.57 ± 0.06	42.2 ± 5	38.8 ± 6
VAMP3 null	164 ± 12	104 ± 7	1.71 ± 0.34	0.44 ± 0.09	138.8 ± 19	81.7 ± 12	0.46 ± 0.04	0.63 ± 0.08	50.2 ± 6	45.5 ± 7

[a] Serum was collected from fed or fasted wild-type or VAMP3 null mice (14 to 16 weeks of age), and the indicated metabolic parameters were determined.

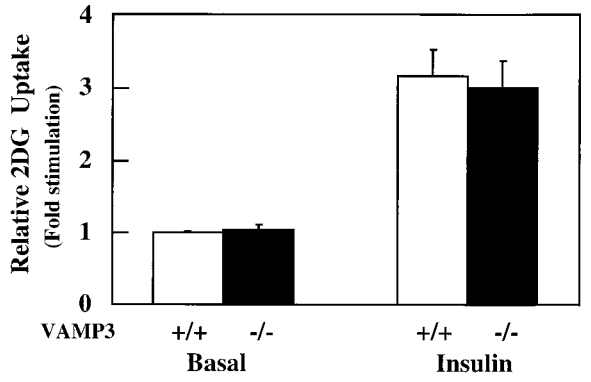

FIG. 5. Insulin-stimulated glucose uptake in isolated primary adipocytes does not differ significantly between wild-type and VAMP3 null mice. Epididymal adipocytes were isolated from 10-week-old males and incubated in the presence or absence of 100 nM insulin for 30 min. 2-Deoxyglucose transport activity was determined as described in Materials and Methods. Results are the average ± standard error from three independent experiments each performed in duplicate.

erance curves were obtained for the VAMP3 null and wild-type mice.

In some circumstances, peripheral tissue insulin resistance can be compensated for by increased insulin secretion. To determine their relative insulin-sensitivities, we subjected these animals to an ITT (Fig. 4B). Following a single intraperitoneal insulin injection, blood glucose values declined up to 30 min and began to recover by 60 min. As observed for glucose tolerance, there was no significant difference between the wild-type and VAMP3 knockout mice. Together, these data indicate that both insulin secretion and peripheral tissue insulin sensitivity were unaltered in the VAMP3 null animals.

Insulin-stimulated glucose transport in isolated primary adipocytes and skeletal muscle is normal in VAMP3-deficient mice. Although whole-body glucose disposal was unaffected in the VAMP3 null mice, it was still possible that secondary metabolic factors might compensate for impaired peripheral tissue glucose transport function. To directly examine glucose transport activity in insulin-responsive tissues, we directly determined insulin-stimulated glucose transport in isolated primary adipocytes (Fig. 5). Consistent with the in vivo results, insulin-stimulated 2-deoxyglucose uptake was essentially identical in adipocytes isolated from wild-type and VAMP3 null mice.

Skeletal muscle accounts for the majority of postprandial glucose disposal in vivo (15). Examination of soleus muscle glucose uptake again demonstrated no significant difference between the wild-type and knockout mice (Fig. 6A). Previous studies have shown that insulin and exercise-contraction recruit different GLUT4 storage compartments in skeletal muscle through distinct signaling pathways (1, 11, 20, 29–31, 39, 50). Since hypoxia in vitro is a commonly used model for exercise-stimulated glucose transport (6, 7, 21, 52), the isolated soleus muscles were also made hypoxic and assayed for glucose transport activity. Even though hypoxia was a weaker activator of glucose uptake than insulin, identical responses were obtained in both wild-type and VAMP3 null mice. Finally, to examine the effect of exercise in vivo, we subjected mice to intense swimming and then determined glucose uptake in isolated EDL muscles (Fig. 6B). Acute swimming led to 2.0- and 2.4-fold increases in glucose transport from the wild-type and VAMP3-deficient mice, respectively. Similarly, insulin stimulation resulted in 2.4-and 3.0-fold increases, respectively. Thus, these data demonstrate that the VAMP3 protein is dispensable for both adipose and skeletal muscle tissue insulin-, hypoxia-, and exercise-contraction-stimulated glucose uptake.

VAMP3 is not essential for phagocytosis. Previous studies observed a recruitment of VAMP3 to sites of phagocytosis, suggesting that VAMP3-containing vesicles may be responsible for the rapid expansion of the membrane structure around the invaginating particle (5). Western blots of clarified lysates demonstrated that VAMP3 was abundant in wild-type BMMs but was undetectable in BMMs from VAMP3 null mice (Fig. 7A). In contrast, low levels of VAMP2 were present in both types of macrophages (Fig. 7A). To determine whether VAMP3 was essential for phagocytosis, we assessed the ability of VAMP3 null and wild-type BMMs to phagocytose zymosan, IgG-opsonized zymosan, or complement opsonized zymosan particles, which engage mannose receptors, Fcγ receptors, or

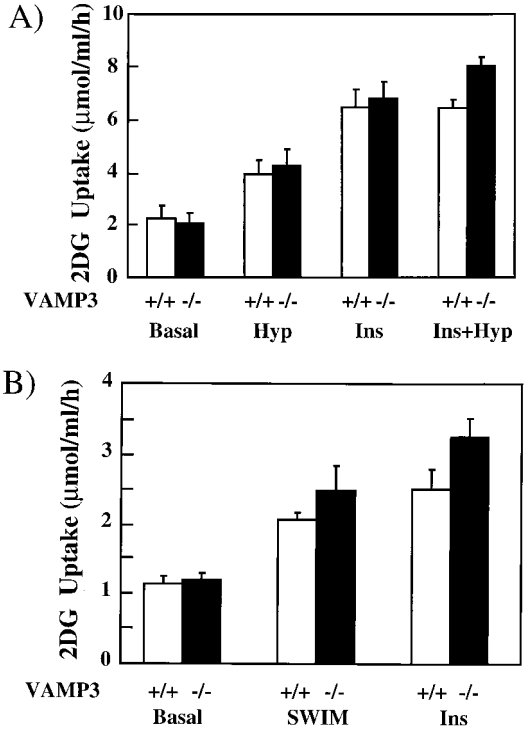

FIG. 6. Insulin-, hypoxia-, and exercise-contraction-stimulated glucose uptake in skeletal muscle is unaffected by the absence of VAMP3. (A) Soleus muscles were isolated from male wild-type or VAMP3-deficient mice and incubated for 45 min under oxygenated or hypoxic (Hyp) conditions with 5 mM glucose at 30°C. The muscles were transferred to oxygenated glucose-free medium and incubated for an additional 15 min prior to the initiation of 2-deoxyglucose uptake as described in Materials and Methods. In parallel, sets of soleus muscle were incubated in the absence or presence of 120 nM insulin (Ins) for 30 min and assayed for 2-deoxyglucose uptake. (B) Mice either remained sedentary or were strenuously exercised by swimming as described in Materials and Methods. EDL muscles were isolated and assayed for 2-deoxyglucose uptake. In parallel, sets of isolated EDL muscles from sedentary mice were incubated with 120 nM insulin for 30 min and assayed for 2-deoxyglucose uptake.

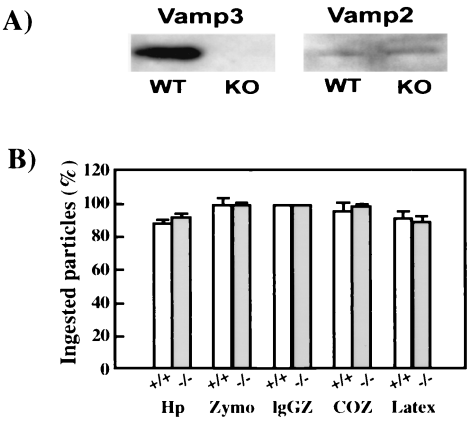

FIG. 7. VAMP3 null BMMs phagocytose inert particles and bacteria. (A) Detection of VAMP2 and VAMP3 in wild-type (WT) and VAMP3 knockout (KO) BMM lysates. (B) *H. pylori* (Hp), zymosan particles (Zymo), IgG-opsonized zymosan (IgGZ), or complement-opsonized zymosan (COZ) was added to cultures of adherent BMMs, and phagocytosis was synchronized by centrifugation. After 30 min at 37°C, ingestion of cell-associated particles was scored as described in Materials and Methods. Data shown are the average ± standard deviation of three independent experiments performed in triplicate. The absence of VAMP3 did not affect particle binding to BMMs, and attachment indices varied by less than 15% for each stimulus (data not shown).

complement receptors, respectively (2). In parallel, BMMs were tested for the ability to ingest the gram-negative bacterium *H. pylori* or latex beads. In all cases, phagocytosis was synchronized by centrifugation and internalization of bound particles was assayed after 30 min at 37°C. As shown in Fig. 7B, we found that VAMP3 null BMMs were indistinguishable from wild-type cells and efficiently ingested all particles and microbes tested regardless of the phagocytic receptor engaged.

VAMP3 is not required for transferrin receptor recycling or pinocytosis. In addition to the trafficking of GLUT4, VAMP3 is distributed throughout the general endosome recycling system and colocalizes with the transferrin receptor (14, 34). We therefore next examined a potential role for VAMP3 in endosome trafficking in isolated primary mouse embryonic fibroblasts. To determine the receptor-mediated endocytosis, the cell surface transferrin receptor was loaded with [^{125}I]transferrin at 4°C and then warmed to 37°C (Fig. 8A). The initial rate of uptake was essentially the same for the wild-type and VAMP3 null fibroblasts. Following internalization, the apotransferrin protein is recycled to the cell surface and released into the medium (26). As observed in Fig. 8B, the rate of transferrin recycling was not significantly different between the wild-type and VAMP3-deficient cells. Similarly, the rate of non-receptor-mediated endocytosis (pinocytosis) was also unaffected by the loss of the VAMP3 protein (Fig. 8C). Taken together, these data demonstrate that VAMP3 is dispensable for multiple aspects of intracellular vesicular trafficking events.

DISCUSSION

It is well established that physiological stimuli leading to enhanced glucose uptake in both striated muscle and adipose tissue primarily result from the recruitment of intracellular compartmentalized GLUT4 protein to the cell surface membrane (31, 37). Several studies have documented the requirement for the t-SNARE proteins syntaxin 4 and SNAP23 to interact with their cognate GLUT4 vesicle protein v-SNAREs, VAMP2 and VAMP3, in the docking and/or fusion process (9, 32, 37, 47, 48). However, the relationship between VAMP2 and VAMP3 function in this process is not entirely clear, as both proteins colocalize with GLUT4 and undergo similar degrees of translocation to the cell surface (33, 47). In addition, expression of dominant-interfering VAMP2 and VAMP3 mutants in 3T3-L1 adipocytes is equally effective in inhibiting insulin-stimulated GLUT4 translocation (37). On the other hand, introduction of various VAMP-specific toxins has suggested that VAMP2 plays the major role in mediating insulin-stimulated GLUT4 translocation (9, 40). Furthermore, endosome ablation using HRP-conjugated transferrin has also provided evidence for VAMP2 but not VAMP3 (32).

To distinguish between the functional properties of VAMP2 and VAMP3 in a physiological context, we used a mouse homologous recombination methodology. Our data clearly demonstrate that complete disruption of VAMP3 expression had no significant effect on whole-body glucose metabolism or insulin-stimulated glucose uptake. Thus, these data unequivocally demonstrate that VAMP3 does not play a significant role in insulin-stimulated glucose transport.

In addition to insulin stimulation, skeletal muscle undergoes a similar degree of exercise-contraction-stimulated GLUT4

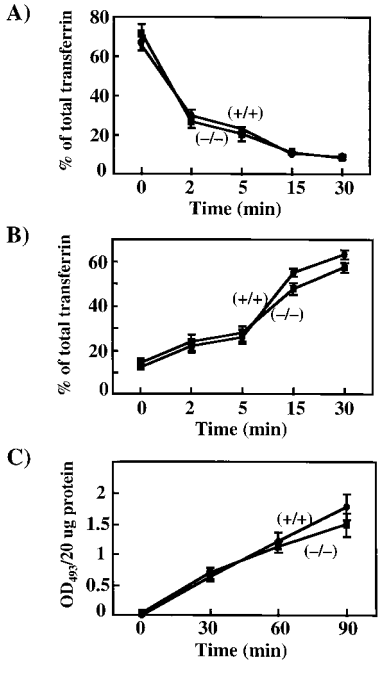

FIG. 8. VAMP3 is not essential for transferrin receptor recycling or pinocytosis in isolated primary mouse embryo fibroblasts. Embryonic fibroblasts from wild-type and VAMP3-deficient mice were depleted of bovine transferrin and labeled with [^{125}I]transferrin (3 nM; 1 μCi/μg) at 4°C for 2 h. Unbound ligand was removed, and then cells were incubated at 37°C for the times indicated. Rates of transferrin internalization (endocytosis) (A), transferrin release (recycling) (B), and HRP uptake (pinocytosis) (C) were determined as described in Materials and Methods. Data shown are the average ± standard deviation of three independent experiments.

translocation and glucose uptake (16, 17, 36, 42, 49, 53). Although the mechanism of exercise-contraction stimulation is not known, this process occurs independently of PI 3-kinase function (30, 31, 50). Similarly, several other stimuli can induce GLUT4 translocation through a PI 3-kinase-independent mechanism including osmotic shock, uncoupling of oxidative phosphorylation, and GTPγS (10, 18, 51). Thus, it has been postulated that these alternative signals mediate GLUT4 translocation through a common signal utilizing a distinct pool of GLUT4 vesicles separate from that of insulin. In this regard, skeletal muscle has been found to contain at least two GLUT4-containing intracellular compartments, one enriched for VAMP2 and the other enriched for VAMP3 (1, 39). More importantly, endosome ablation of the VAMP3-containing GLUT4 population, though having no effect on insulin stimulation, was found to prevent GTPγS-stimulated GLUT4 translocation (35). Surprisingly, however, the VAMP3 null mice also did not display any impairment in exercise-contraction-stimulated glucose uptake. Thus, our data indicate that VAMP3 is dispensable for both insulin- and exercise-contraction-stimulated glucose uptake in vivo.

In addition to the potential role in GLUT4 translocation, VAMP3 has also been suggested to be involved in receptor and non-receptor-mediated endocytosis (5, 22). Our data clearly demonstrate that neither phagocytosis, transferrin receptor recycling, nor fluid-phase endocytosis (pinocytosis) was affected by the loss of VAMP3. There are several possible mechanisms that could account for these discrepancies. The most likely is that VAMP2 or some other v-SNARE protein can compensate for the genetic loss of VAMP3 during muscle and adipose tissue development. Alternatively, VAMP3 function may simply be redundant to ensure fidelity of GLUT4 and endosome trafficking. In either case, the completely normal intracellular trafficking of a variety of membrane processes in VAMP3 null mice provides a direct demonstration that VAMP3 is not essential for general endosome trafficking, phagocytosis, or insulin- or exercise-contraction-stimulated glucose transport activity in vivo.

ACKNOWLEDGMENTS

We thank Diana Boeglin for assistance with the glucose tolerance and insulin tolerance tests. We also thank Ann Davis (Bayer) for helpful discussion the design of the VAMP3 targeting vector.

This work was supported by research grants DK33823, DK55811, and DK25295 from the National Institutes of Health. S.M. is a recipient of a postdoctoral fellowship (Formación de Personal Investigador) from the Ministerio de Educación y Cultura, Spain. L.-A.A. is a recipient of a Merit Review award from the Veterans Administration.

REFERENCES

1. **Aledo, J. C., L. Lavoie, A. Volchuck, S. R. Keller, A. Klip, and H. S. Hundal.** 1997. Identification and characterization of two distinct intracellular GLUT4 pools in rat skeletal muscle: evidence for an endosomal and an insulin-sensitive GLUT4 compartment. Biochem. J. **325:**727–732.
2. **Allen, L. A., and A. Aderem.** 1996. Molecular definition of distinct cytoskeletal structures involved in complement-and Fc receptor-mediated phagocytosis in macrophages. J. Exp. Med. **184:**627–637.
3. **Allen, L. A., L. S. Schlesinger, and B. Kang.** 2000. Virulent strains of Helicobacter pylori demonstrate delayed phagocytosis and stimulate homotypic phagosome fusion in macrophages. J. Exp. Med. **191:**115–128.
4. **Allen, L. H., and A. Aderem.** 1995. A role for MARCKS, the alpha isozyme of protein kinase C and myosin I in zymosan phagocytosis by macrophages. J. Exp. Med. **182:**829–840.
5. **Bajno, L., X. R. Peng, A. D. Schreiber, H. P. Moore, W. S. Trimble, and S. Grinstein.** 2000. Focal exocytosis of VAMP3-containing vesicles at sites of phagosome formation. J. Cell Biol. **149:**697–706.
6. **Brozinick, J. T., Jr., S. C. McCoid, T. H. Reynolds, C. M. Wilson, R. W. Stevenson, S. W. Cushman, and E. M. Gibbs.** 1997. Regulation of cell surface GLUT4 in skeletal muscle of transgenic mice. Biochem. J. **321:**75–81.
7. **Cartee, G. D., A. G. Douen, T. Ramlal, A. Klip, and J. O. Holloszy.** 1991. Stimulation of glucose transport in skeletal muscle by hypoxia. J. Appl. Physiol. **70:**1593–1600.
8. **Ceresa, B. P., A. W. Kao, S. R. Santeler, and J. E. Pessin.** 1998. Inhibition of clathrin-mediated endocytosis selectively attenuates specific insulin receptor signal transduction pathways. Mol. Cell. Biol. **18:**3862–3870.
9. **Cheatham, B., A. Volchuk, C. R. Kahn, L. Wang, C. J. Rhodes, and A. Klip.** 1996. Insulin-stimulated translocation of GLUT4 glucose transporters requires SNARE-complex proteins. Proc. Natl. Acad. Sci. USA **93:**15169–15173.
10. **Chen, D., J. S. Elmendorf, A. L. Olson, X. Li, H. S. Earp, and J. E. Pessin.** 1997. Osmotic shock stimulates GLUT4 translocation in 3T3L1 adipocytes by a novel tyrosine kinase pathway. J. Biol. Chem. **272:**27401–27410.
11. **Coderre, L., K. V. Kandror, G. Vallega, and P. F. Pilch.** 1995. Identification and characterization of an exercise-sensitive pool of glucose transporters in skeletal muscle. J. Biol. Chem. **270:**27584–27588.
12. **Czech, M. P.** 1995. Molecular actions of insulin on glucose transport. Annu. Rev. Nutr. **15:**441–471.
13. **Daro, E., D. Sheff, M. Gomez, T. Kreis, and I. Mellman.** 1997. Inhibition of endosome function in CHO cells bearing a temperature-sensitive defect in the coatomer (COPI) component e-COP. J. Cell Biol. **139:**1747–1759.
14. **Daro, E., P. V. Sluijs, T. Galli, and I. Mellman.** 1996. Rab4 and cellubrevin define different early endosome populations on the pathway of transferrin receptor recycling. Proc. Natl. Acad. Sci. USA **93:**9559–9564.
15. **DeFronzo, R. A., E. Jacot, E. Jequier, E. Maeder, J. Wahren, and J. P. Felber.** 1981. The effect of insulin on the disposal of intravenous glucose. Results from indirect calorimetry and hepatic and femoral venous catheterization. Diabetes **30:**1000–1007.
16. **Douen, A. G., T. Ramlal, A. Klip, D. A. Young, G. D. Cartee, and J. O. Holloszy.** 1989. Exercise-induced increase in glucose transporters in plasma membranes of rat skeletal muscle. Endocrinology **24:**449–454.
17. **Douen, A. G., T. Ramlal, S. Rastogi, P. J. Bilan, G. D. Cartee, M. Vranic, J. O. Holloszy, and A. Klip.** 1990. Exercise induces recruitment of the "insulin-responsive glucose transporter." Evidence for distinct intracellular insulin- and exercise-recruitable transporter pools in skeletal muscle. J. Biol. Chem. **265:**13427–13430.
18. **Elmendorf, J. S., D. Chen, and J. E. Pessin.** 1998. Guanosine 5′-0-(3-thiotriphosphate) (GTPgammaS) stimulation of GLUT4 translocation is tyrosine kinase-dependent. J. Biol. Chem. **273:**13289–13296.
19. **Enrique-Tarancon, G., L. Marti, N. Morin, J. M. Lizcano, M. Unzeta, L. Sevilla, M. Camps, M. Palacin, X. Testar, C. Carpene, and A. Zorzano.** 1998. Role of semicarbazide-sensitive amine oxidase on glucose transport and GLUT4 recruitment to the cell surface in adipose cells. J. Biol. Chem. **273:**8025–8032.
20. **Goodyear, L. J., F. Giorgino, T. W. Balon, G. Condorelli, and R. J. Smith.** 1995. Effects of contractile activity on tyrosine phosphoproteins and PI 3-kinase activity in rat skeletal muscle. Am. J. Physiol. **268:**E987–E995.
21. **Gulve, E. A., J. M. Ren, B. A. Marshall, J. Gao, P. A. Hansen, J. O. Holloszy, and M. Mueckler.** 1994. Glucose transport activity in skeletal muscles from transgenic mice overexpressing GLUT1. Increased basal transport is associated with a defective response to diverse stimuli that activate GLUT4. J. Biol. Chem. **269:**18366–18370.
22. **Hackam, D. J., O. D. Rotstein, C. Sjolin, A. D. Schreiber, W. S. Trimble, and S. Grinstein.** 1998. v-SNARE-dependent secretion is required for phagocytosis. Proc. Natl. Acad. Sci. USA **95:**11691–11696.
23. **Hansen, P. A., E. A. Gulve, B. A. Marshall, J. Gao, J. E. Pessin, J. O. Holloszy, and M. Mueckler.** 1995. Skeletal muscle glucose transport and metabolism are enhanced in transgenic mice overexpressing the Glut4 glucose transporter. J. Biol. Chem. **270:**1679–1684.
24. **Heesemann, J., and R. Laufs.** 1985. Double immunofluorescence microscopic technique for accurate differentiation of extracellularly and intracellularly located bacteria in cell culture. J. Clin. Microbiol. **22:**168–175.
25. **Hogan, B., R. Beddington, F. Costantini, and E. Lacy.** 1994. Manipulating the mouse embryo, 2nd ed., Cold Spring Harbor Laboratory Press, Cold Spring Harbor, N.Y.
26. **Hopkins, C. R., and I. S. Trowbridge.** 1983. Internalization and processing of transferrin and the transferrin receptor in human carcinoma A431 cells. J. Cell Biol. **97:**508–521.
27. **Kandror, K. V., and P. F. Pilch.** 1996. Compartmentalization of protein traffic in insulin-sensitive cells. Am. J. Physiol. **271:**E1–E14.
28. **Kao, A. W., B. P. Ceresa, S. R. Santeler, and J. E. Pessin.** 1998. Expression of a dominant interfering dynamin mutant in 3T3L1 adipocytes inhibits GLUT4 endocytosis without affecting insulin signaling. J. Biol. Chem. **273:**25450–25457.
29. **Koval, J. A., K. Maezono, M. E. Patti, M. Pendergrass, R. A. DeFronzo, and L. J. Mandarino.** 1999. Effects of exercise and insulin on insulin signaling proteins in human skeletal muscle. Med. Sci. Sports Exerc. **31:**998–1004.
30. **Lee, A. D., P. A. Hansen, and J. O. Holloszy.** 1995. Wortmannin inhibits

insulin-stimulated but not contraction-stimulated glucose transport activity in skeletal muscle. FEBS Lett. **361:**51–54.
31. **Lund, S., G. D. Holman, O. Schmitz, and O. Pedersen.** 1995. Contraction stimulates translocation of glucose transporter GLUT4 in skeletal muscle through a mechanism distinct from that of insulin. Proc. Natl. Acad. Sci. USA **92:**5817–5821.
32. **Martin, L. B., A. Shewan, C. A. Millar, G. W. Gould, and D. E. James.** 1998. Vesicle-associated membrane protein 2 plays a specific role in the insulin-dependent trafficking of the facilitative glucose transporter GLUT4 in 3T3–L1 adipocytes. J. Biol. Chem. **273:**1444–1452.
33. **Martin, S., J. Tellam, C. Livingstone, J. W. Slot, G. W. Gould, and D. E. James.** 1996. The glucose transporter (GLUT-4) and vesicle-associated membrane protein-2 (VAMP-2) are segregated from recycling endosomes in insulin-sensitive cells. J. Cell Biol. **134:**625–635.
34. **McMahon, H. T., Y. A. Ushkaryov, L. Edelmann, E. Link, T. Binz, H. Niemann, R. Jahn, and T. C. Sudhof.** 1993. Cellubrevin is a ubiquitous tetanus-toxin substrate homologous to a putative synaptic vesicle fusion protein. Nature **364:**346–349.
35. **Millar, C. A., A. Shewan, G. R. Hickson, D. E. James, and G. W. Gould.** 1999. Differential regulation of secretory compartments containing the insulin-responsive glucose transporter 4 in 3T3–L1 adipocytes. Mol. Biol. Cell. **10:** 3675–3688.
36. **Nesher, R., I. E. Karl, and D. M. Kipnis.** 1985. Dissociation of effects of insulin and contraction on glucose transport in rat epitrochlearis muscle. Am. J. Physiol. **249:**C226–C232.
37. **Olson, A. L., J. B. Knight, and J. E. Pessin.** 1997. Syntaxin 4, VAMP2, and/or VAMP3/cellubrevin are functional target membrane and vesicle SNAP receptors for insulin-stimulated GLUT4 translocation in adipocytes. Mol. Cell. Biol. **17:**2425–2435.
38. **Pessin, J. E., D. C. Thurmond, J. S. Elmendorf, K. J. Coker, and S. Okada.** 1999. Molecular basis of insulin-stimulated GLUT4 vesicle trafficking. Location! Location! Location! J. Biol. Chem. **274:**2593–2596.
39. **Ploug, T., B. van Deurs, H. Ai, S. W. Cushman, and E. Ralston.** 1998. Analysis of GLUT4 distribution in whole skeletal muscle fibers: identification of distinct storage compartments that are recruited by insulin and muscle contractions. J. Cell Biol. **142:**1429–1446.
40. **Randhawa, V. K., P. J. Bilan, Z. A. Khayat, N. Daneman, Z. Liu, T. Ramlal, A. Volchuk, X. R. Peng, T. Coppola, R. Regazzi, W. S. Trimble, and A. Klip.** 2000. VAMP2, but not VAMP3/cellubrevin, mediates insulin-dependent incorporation of GLUT4 into the plasma membrane of L6 myoblasts. Mol. Biol. Cell **11:**2403–2417.
41. **Rea, S., and D. E. James.** 1997. Moving GLUT4. The biogenesis and trafficking of GLUT4 storage vesicles. Diabetes **46:**1667–1677.
42. **Richter, E. A., T. Ploug, and H. Galbo.** 1985. Increased muscle glucose uptake after exercise. No need for insulin during exercise. Diabetes **34:**1041–1048.
43. **Ryder, J. W., Y. Kawano, D. Galuska, R. Fahlman, H. Wallberg-Henriksson, M. J. Charron, and J. R. Zierath.** 1999. Postexercise glucose uptake and glycogen synthesis in skeletal muscle from GLUT4-deficient mice. FASEB J. **13:**2246–2256.
44. **Slot, J. W., H. J. Geuze, S. Gigengack, D. E. James, and G. E. Lienhard.** 1991a. Translocation of the glucose transporter GLUT4 in cardiac myocytes of the rat. Proc. Natl. Acad. Sci. USA **88:**7815–7819.
45. **Slot, J. W., H. J. Geuze, S. Gigengack, G. E. Lienhard, and D. E. James.** 1991b. Immuno-localization of the insulin regulatable glucose transporter in brown adipose tissue of the rat. J. Cell Biol. **113:**123–135.
46. **Thurmond, D. C., B. P. Ceresa, S. Okada, J. S. Elmendorf, K. Coker, and J. E. Pessin.** 1998. Regulation of insulin-stimulated GLUT4 translocation by Munc18c in 3T3L1 adipocytes. J. Biol. Chem. **273:**33876–33883.
47. **Volchuk, A., R. Sargeant, S. Sumitani, Z. Liu, L. He, and A. Klip.** 1995. Cellubrevin is a resident protein of insulin-sensitive GLUT4 glucose transporter vesicles in 3T3–L1 adipocytes. J. Biol. Chem. **270:**8233–8240.
48. **Volchuk, A., Q. Wang, H. S. Ewart, Z. Liu, L. He, M. K. Bennett, and A. Klip.** 1996. Syntaxin 4 in 3T3–L1 adipocytes: regulation by insulin and participation in insulin-dependent glucose transport. Mol. Biol. Cell **7:**1075–1082.
49. **Wallberg-Henriksson, H., and J. O. Holloszy.** 1985. Activation of glucose transport in diabetic muscle: responses to contraction and insulin. Am. J. Physiol. **249:**C233–C237.
50. **Yeh, J. I., E. A. Gulve, L. Rameh, and M. J. Birnbaum.** 1995. The effects of wortmannin on rat skeletal muscle. Dissociation of signaling pathways for insulin- and contraction-activated hexose transport. J. Biol. Chem. **270:**2107–2111.
51. **Zhang, J. Z., A. Behrooz, and F. Ismail-Beigi.** 1999. Regulation of glucose transport by hypoxia. Am. J. Kidney Dis. **34:**189–202.
52. **Zierath, J. R., K. L. Houseknecht, L. Gnudi, and B. B. Kahn.** 1997. High-fat feeding impairs insulin-stimulated GLUT4 recruitment via an early insulin-signaling defect. Diabetes **46:**215–223.
53. **Zorzano, A., T. W. Balon, M. N. Goodman, and N. B. Ruderman.** 1986. Additive effects of prior exercise and insulin on glucose and AIB uptake by rat muscle. Am. J. Physiol. **251:**E21–E26.